USE OF SMA BARS TO ENHANCE THE SEISMIC PERFORMANCE OF SMA BRACED RC FRAMES

Mohamed E. Meshaly[1], Maged A. Youssef*[1], Hamdy M. Abou Elfath[2]

[1] *Department of Civil and Environmental Engineering, Western University, London, Ontario, Canada, N6A 5B9*
[2] *Department of Structural Engineering, Alexandria University, Alexandria, Egypt*

(Received , Revised , Accepted)

Abstract. Shape Memory Alloy (SMA) braces can be used to reduce seismic residual deformations observed in steel braced Reinforced Concrete (RC) frames. To further enhance the seismic performance of these frames, the use of SMA bars to reinforce their beams is investigated in this paper. Three-story and nine-story SMA-braced RC frames are designed utilizing regular steel reinforcing bars. Their seismic performance is examined using twenty seismic ground motions. The frames are then re-designed using SMA reinforcing bars. Different design alternatives representing different locations for the SMA reinforcing bars are considered. The optimum locations for the SMA bars are identified after analysing the design alternatives. The seismic performance of these frames has indicated better deformability when SMA bars are used in the beams.

Keywords: SMA, residual deformations, braced frames, seismic performance, reinforced concrete, design alternatives.

1. Introduction

McCormick and DesRoches (2003) analytically evaluated the effectiveness of using large diameter superelastic SMA bars as bracing members for existing RC frames. The SMA Bracing (SMAB) members were found effective in reducing the residual story drift and column rotation as compared to traditional steel brace members. Auricchio et al. (2006) compared the seismic performance of steel braces and superelastic SMABs when implemented in three- and six-story steel buildings. They found that buildings with SMABs had reduced residual drifts. Asgarian and Moradi (2011) found that implementing the SMA braces can lead to reduction in residual roof displacements as compared to buckling restrained braced frames.

Youssef et al. (2008) experimentally investigated the seismic behaviour of beam-column joints reinforced with superelastic SMA bars. Their results indicated significant reduction in seismic residual displacements. Saiidi and Wang (2006) observed that superelastic SMA RC columns are capable of dissipating substantive amount of seismic energy with almost no residual deformations. Small-scale concrete beams with SMA reinforcement were tested by Saiidi et al. (2007) and showed that the average residual displacement in the SMA reinforced beams was less than one-fifth of that of the steel reinforced beams. Saiidi et al. (2009) used Engineering Cementitious Composites (ECC) to repair damaged SMA RC columns and showed that the repaired columns were able to recover nearly all of their post-yield deformations.

* Corresponding author, Associate Professor, Tel.: +1 519 661-2111 Ext. 88661; Fax: +1 519 661-3779, E-mail address: youssef@uwo.ca

Alam et al. (2009) used superelastic SMA RC elements in moment resisting frames and concluded that SMA RC frames exhibit better deformability than steel RC frames because of their re-centring capability. Youssef and Elfeki (2012) defined the optimum locations of SMA reinforcing bars in a typical RC frames to achieve reduced seismic residual deformations. The present study evaluates the potential for using SMA bars and SMA braces in concrete frames.

2. Frame design

Three- and nine-story RC office buildings were considered. The exterior frames of both buildings were assumed to be braced using a stacked chevron (inverted-V) pattern. The story height was 3.6 m.

Floor plan and elevations of both buildings are shown in Fig. 1. The two buildings were designed according to ACI (2008) and the international building code (IBC 2009). The buildings were assumed to be located in Berkley, California with site class C. The design spectral response acceleration parameters at short period (S_{DS}) and one second (S_{D1}) were 1.10g and 0.59g, respectively. A response modification factor (R), an over-strength factor (Ω_o), and deflection amplification factor (C_d) of 8, 2.5, and 5, respectively, were used. The design dead loads included weight of the concrete slab (4.32 kN/m^2), flooring (1.44 kN/m^2) and partition walls (0.96 kN/m^2). The design base shears were found to be 507 kN and 670 kN for the three- and nine-story frames, respectively. The frames were designed for critical combinations of dead, live, and seismic loadings.

Material properties for steel and SMA are summarised in Table 1. The SMABs consist of rigid elements connected to the frame using SMA bars (Fig. 2). Similar braces were used by Auricchio et al. (2006). A proposed connection detail is shown in Fig. 3. The required length and areas of the SMA bars for the three- and nine-story frames are shown in Table 2. Choice of the number and diameter of SMA bars is done such that they do not experience buckling.

Table 1: Material properties

Initial modulus of elasticity of steel	200,000 MPa
Initial modulus of elasticity of SMA	68,200 MPa
Yield strength of reinforcing steel bars	413 MPa
Austenite to martensite starting stress (σ_S^{AS})	480 MPa
Austenite to martensite finishing stress (σ_F^{AS})	540 MPa
Martensite to austenite starting stress (σ_S^{SA})	260 MPa
Martensite to austenite finishing stress (σ_F^{SA})	120 MPa
Maximum recoverable strain (ε_L)	6.2 %
Compressive strength of concrete	27.57 MPa
Tensile strength of concrete	2.75 MPa

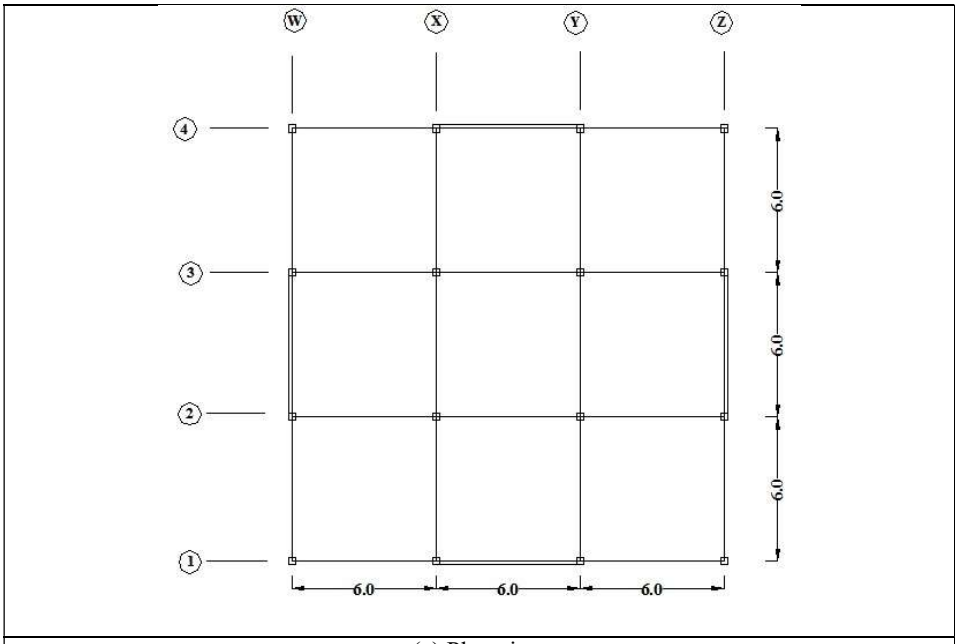

(a) Plan view

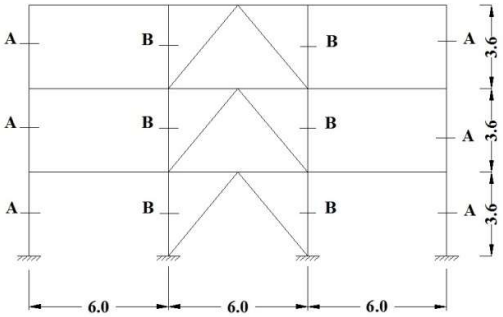

(b) Elevation of the three-story building

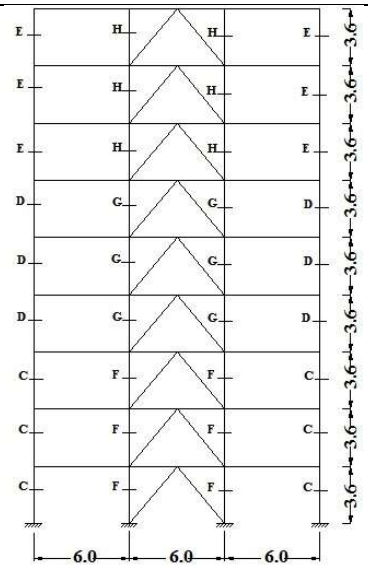

(c) Elevation of the nine-story building

Fig. 1 RC braced frames (All dimensions are in meters)

Four different types of RC frames have been considered in this study: (1) Frame 1: a three-story frame equipped with SMAB and reinforced with steel bars, (2) Frames 2-1 to 2-6: Frame 1 design was modified by using SMA reinforcing bars at a number of locations, (3) Frame 3: a nine-story frame equipped with SMAB and reinforced with steel bars, (4) Frames 4-1 to 4-18: Frame 3 design was modified to include SMA reinforcing bars at a number of locations.

Details of the reinforced concrete beams and columns are shown in Fig. 4. The SMA reinforced sections were designed assuming that the austenite to martensite starting stress defines the SMA yielding point. A schematic diagram that defines the potential locations of SMA reinforcing bars is shown in Fig. 5. Locations BE represent potential plastic hinge locations at the beam-column connections. A plastic hinge might also develop at location BM. The design alternatives for Frames 2 and 4 are summarized in Tables 3 and 4, respectively.

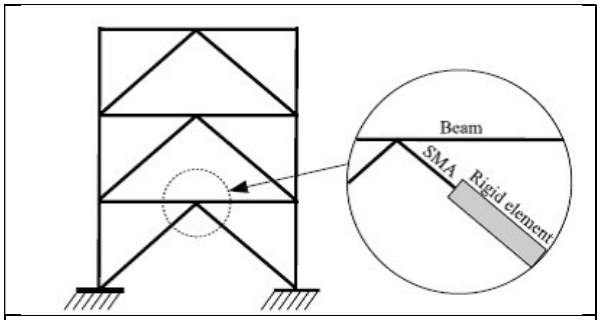

Fig. 2 Components of SMA Brace

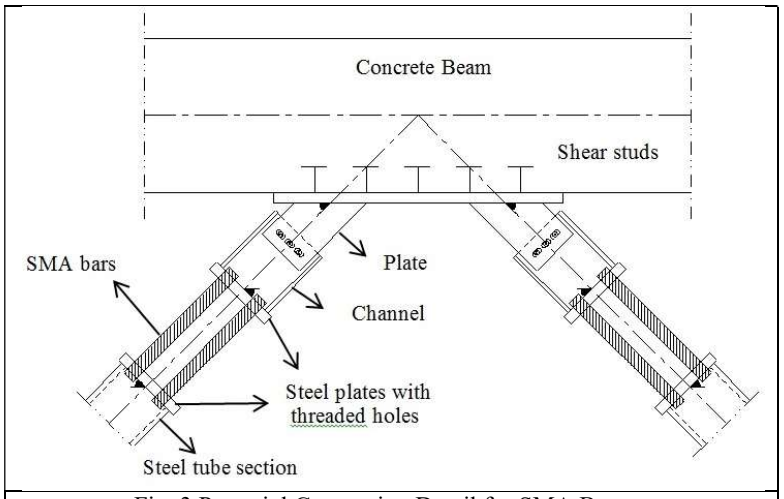

Fig. 3 Potential Connection Detail for SMA Braces

Table 2: SMA details for braces of the three- and nine-story frames

Frame	Three-story		Nine-story	
Story	Length (mm)	Area (mm^2)	Length (mm)	Area (mm^2)
1	650	641.90	650	846.76
2	650	539.35	650	838.43
3	650	326.39	650	815.28
4	-	-	650	774.07
5	-	-	650	711.34
6	-	-	650	625.00
7	-	-	650	512.73
8	-	-	650	372.45
9	-	-	650	202.08

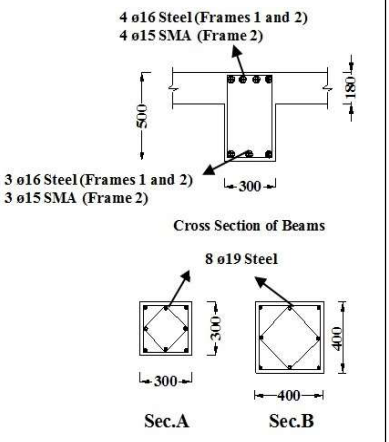

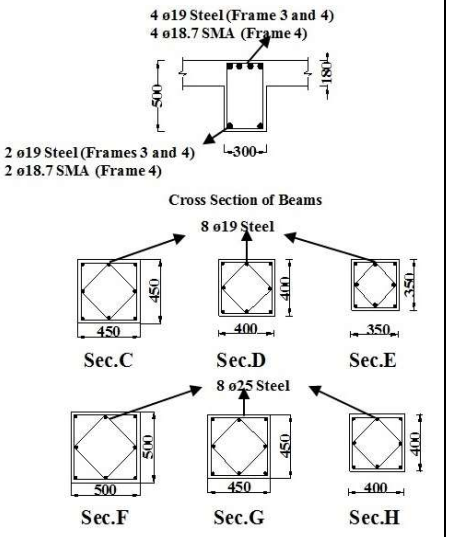

(a) Details of Frames 1 and 2 (b) Details of Frames 3 and 4

Fig. 4 Sections of the designed frame

Table 3: Location of SMA bars for Frames 2-1 to 2-6

Frame	Location of SMA reinforcing bars		
	1st story	2nd story	3rd story
2-1	BE	-	-
2-2	BE+BM	-	-
2-3	BE	BE	-
2-4	BE+BM	BE+BM	-
2-5	BE	BE	BE
2-6	BE+BM	BE+BM	BE+BM

Table 4: Location of SMA bars for Frames 4-1 to 4-18

Frame	Location of SMA reinforcing bars								
	1st story	2nd story	3rd story	4th story	5th story	6th story	7th story	8th story	9th story
4-1	BE	-	-	-	-	-	-	-	-
4-2	BE+BM	-	-	-	-	-	-	-	-
4-3	BE	BE	-	-	-	-	-	-	-
4-4	BE+BM	BE+BM	-	-	-	-	-	-	-
4-5	BE	BE	BE	-	-	-	-	-	-
4-6	BE+BM	BE+BM	BE+BM	-	-	-	-	-	-
4-7	BE	BE	BE	BE	-	-	-	-	-
4-8	BE+BM	BE+BM	BE+BM	BE+BM	-	-	-	-	-
4-9	BE	BE	BE	BE	BE	-	-	-	-
4-10	BE+BM	BE+BM	BE+BM	BE+BM	BE+BM	-	-	-	-
4-11	BE	BE	BE	BE	BE	BE	-	-	-
4-12	BE+BM	BE+BM	BE+BM	BE+BM	BE+BM	BE+BM	-	-	-
4-13	BE	BE	BE	BE	BE	BE	BE	-	-
4-14	BE+BM	BE+BM	BE+BM	BE+BM	BE+BM	BE+BM	BE+BM	-	-
4-15	BE	BE	BE	BE	BE	BE	BE	BE	-
4-16	BE+BM	BE+BM	BE+BM	BE+BM	BE+BM	BE+BM	BE+BM	BE+BM	-
4-17	BE	BE	BE	BE	BE	BE	BE	BE	BE
4-18	BE+BM	BE+BM	BE+BM	BE+BM	BE+BM	BE+BM	BE+BM	BE+BM	BE+BM

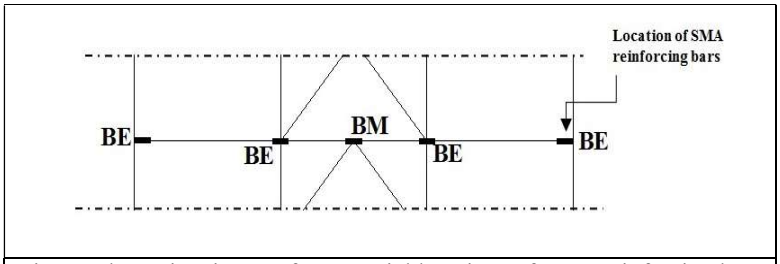

Fig. 5 Schematic Diagram for potential locations of SMA reinforcing bars

Numerous models can be used to estimate the length of the plastic hinge (L_p) for steel RC beams. Alam et al. (2008) investigated the applicability of these models for SMA RC beams. Equation 1 by Paulay and Priestley (1992) was found to provide good estimates for the plastic hinge length of SMA RC members.

$$L_p = 0.08\,L + 0.022\,d_b f_y \quad (1)$$

where L is the span length in mm, d_b is the bar diameter in mm, and f_y is the yield strength of the bar in MPa.

The length of the plastic hinge for typical beams was calculated as 640 mm and 680 mm for SMA bar diameters of 15.0 mm and 18.7 mm, respectively. SMA reinforcing bars were assumed to be connected with steel bars by mechanical couplers as shown in Fig. 6.

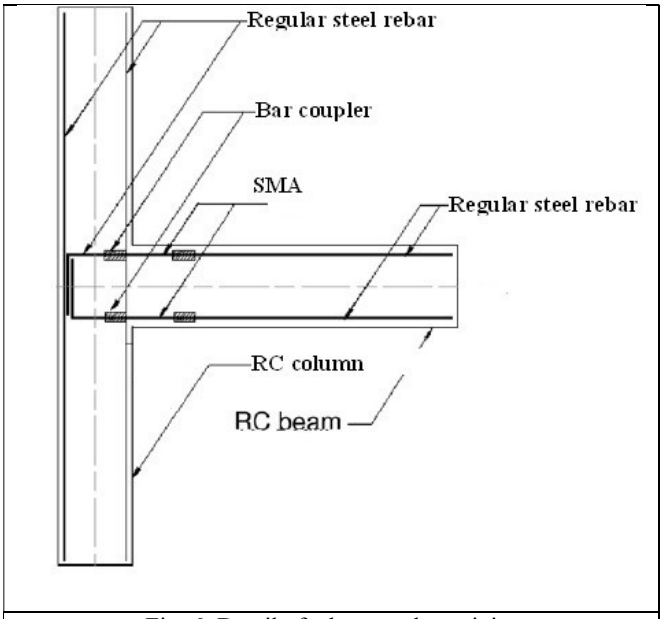

Fig. 6: Detail of a beam column joint

3. Modelling

The frames were modelled using the SeismoStruct computer program (SeismoSoft 2009). Concrete was modelled using a uniaxial nonlinear constant confinement concrete model that follows the constitutive relationship proposed by Mander et al. (1988) and the cyclic rules proposed by Martinez-Rueda and Elnashai (1997). Beams and columns were divided into four displacement-based elements that utilize the fibre modelling approach to capture the spread of inelasticity along the member length. The sectional stress-strain state is obtained through the integration of the nonlinear uniaxial stress-strain response of the individual fibres forming the cross-section.

SMA is modelled using the uniaxial model proposed by Auricchio and Sacco (1997) and shown in Fig. 7. The model assumes a constant stiffness for both the fully austenite and fully martensite phases. The parameters used to define the material model in the program are: austenite to martensite starting stress (σ_S^{AS}), austenite to martensite finishing stress (σ_F^{AS}), martensite to austenite starting stress (σ_S^{SA}), martensite to austenite finishing stress (σ_F^{SA}), maximum recoverable strain (ε_L).

The structural mass is assumed to be lumped at the beam column joints. A time step of 0.005 second was used for the dynamic analysis. The effect of the geometric non-linearity (P-Δ effect)

was considered. Vamvatsikos and Cornell (2004) recommended the use of 20 records from three earthquakes (1979 Imperial Valley, 1987 Superstition Hills, and 1989 Loma Prieta) to analyze low- and mid-rise buildings. The characteristics of those 20 records are summarized in Table 5. The records cover a wide range of frequency contents and durations and were utilized in the present study. Scaled versions of the twenty records with peak ground accelerations PGA of 0.5g, 0.75g, 1.0g, and 1.25g were used for the dynamic analysis. The response parameters considered in the evaluation of the frames are: the damage mechanism, the roof drift ratio, the residual roof drift ratio, and the maximum story drift ratio.

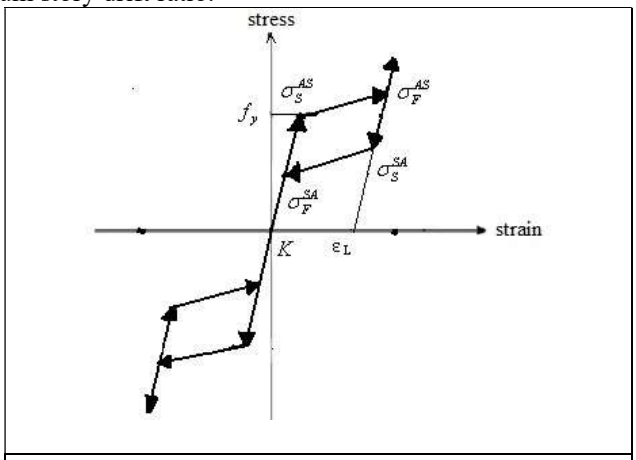

Fig. 7: The superelastic SMA model (Auricchio et al. 2006)

Table 5: Selected Earthquake Ground Motion Records

Record No.	Event	Year	Record Station	Φ[1]	M*[2]	R*[3](Km)	PGA(g)
1	Imperial Valley	1979	Cucapah	85	6.9	23.6	0.309
2	Imperial Valley	1979	Chihuahua	282	6.5	28.7	0.254
3	Imperial Valley	1979	El Centro Array # 13	140	6.5	21.9	0.117
4	Imperial Valley	1979	El Centro Array # 13	230	6.5	21.9	0.139
5	Imperial Valley	1979	Plaster City	45	6.5	31.7	0.042
6	Imperial Valley	1979	Plaster City	135	6.5	31.7	0.057
7	Imperial Valley	1979	Westmoreland Fire Sta.	90	6.5	15.1	0.074
8	Imperial Valley	1979	Westmoreland Fire Sta.	180	6.5	15.1	0.110
9	Loma Prieta	1989	Agnews State Hospital	90	6.9	28.2	0.159
10	Loma Prieta	1989	Anderson Dam	270	6.9	21.4	0.244
11	Loma Prieta	1989	Coyote Lake Dam	285	6.5	22.3	0.179
12	Loma Prieta	1989	Hollister Diff. Array	255	6.9	25.8	0.279
13	Loma Prieta	1989	Hollister Diff. Array	165	6.9	25.8	0.269
14	Loma Prieta	1989	Holister South & Pine	0	6.9	28.8	0.371
15	Loma Prieta	1989	Sunnyvale Colton Ave	270	6.9	28.8	0.207
16	Loma Prieta	1989	Sunnyvale Colton Ave	360	6.9	28.8	0.209
17	Superstition Hill	1987	Wildlife Liquefaction Array	90	6.7	24.4	0.180
18	Superstition Hill	1987	Wildlife Liquefaction Array	360	6.7	24.4	0.200
19	Loma Prieta	1989	WAHO	0	6.9	16.9	0.370
20	Loma Prieta	1989	WAHO	90	6.9	16.9	0.638

[1] Component, [2] Moment Magnitudes, [3] Closest Distances to Fault Rupture

4. Seismic Response

4.1 Failure Mechanism

The sequence of brace yielding and core concrete crushing of Frames 1 and 3 at different PGA values are shown in Figs. 8 and 9, respectively. These results are for records 18 and 14 for Frames 1 and 3, respectively, and represent typical damage. Yielding of brace members was observed for all of the considered PGA values. For both frames, concrete crushing was observed at PGA of 0.75g in the beams and at PGA of 1.00g in the columns. Both frames were severely damaged at PGA of 1.25g.

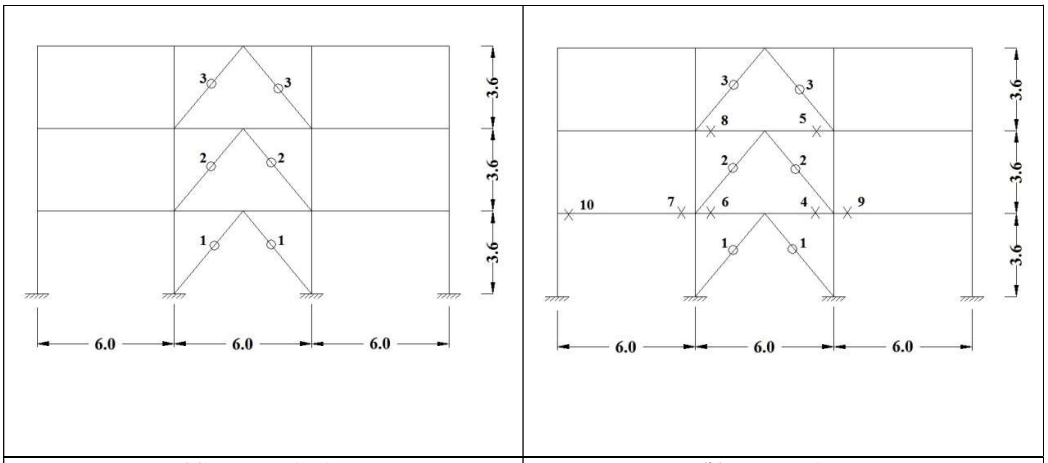

(a) PGA = 0.50g | (b) PGA = 0.75g

(c) PGA = 1.00g | (d) PGA = 1.25g

x : core concrete crushing o : yielding of bracing

Fig. 8: The sequence of core concrete crushing and yielding of bracing of Frame 1 (record no. 18)

4.2 Comparison of the SMA design alternatives

Frames 2-1 to 2-6 and 4-1 to 4-18 were found to have almost the same map of yielding and crushing as Frames 1 and 3, respectively. Considering records 18 and 14, the residual roof

displacements of Frames 1 and 3 were 20 mm and 106 mm, respectively. The residual roof displacements of Frames 2-1 to 2-6 were 8.5, 7.5, 8.5, 4.5, 17, and 2.0 mm, respectively. Their values for Frames 4-1 to 4-18 were 103, 102, 107, 100, 107, 100, 100, 95, 92, 89, 87, 83, 80, 76, 71, 67, 70, and 64 mm, respectively.

It is clear that some of the design alternatives (Frame 2-5, Frames 4-1 to 4-11) do not provide a major advantage over Frames 1 and 3. Frames 2-6 and 4-18 achieved the lowest residual roof drift displacement when compared to Frames 1 and 3, respectively. Similar results were obtained for the other records.

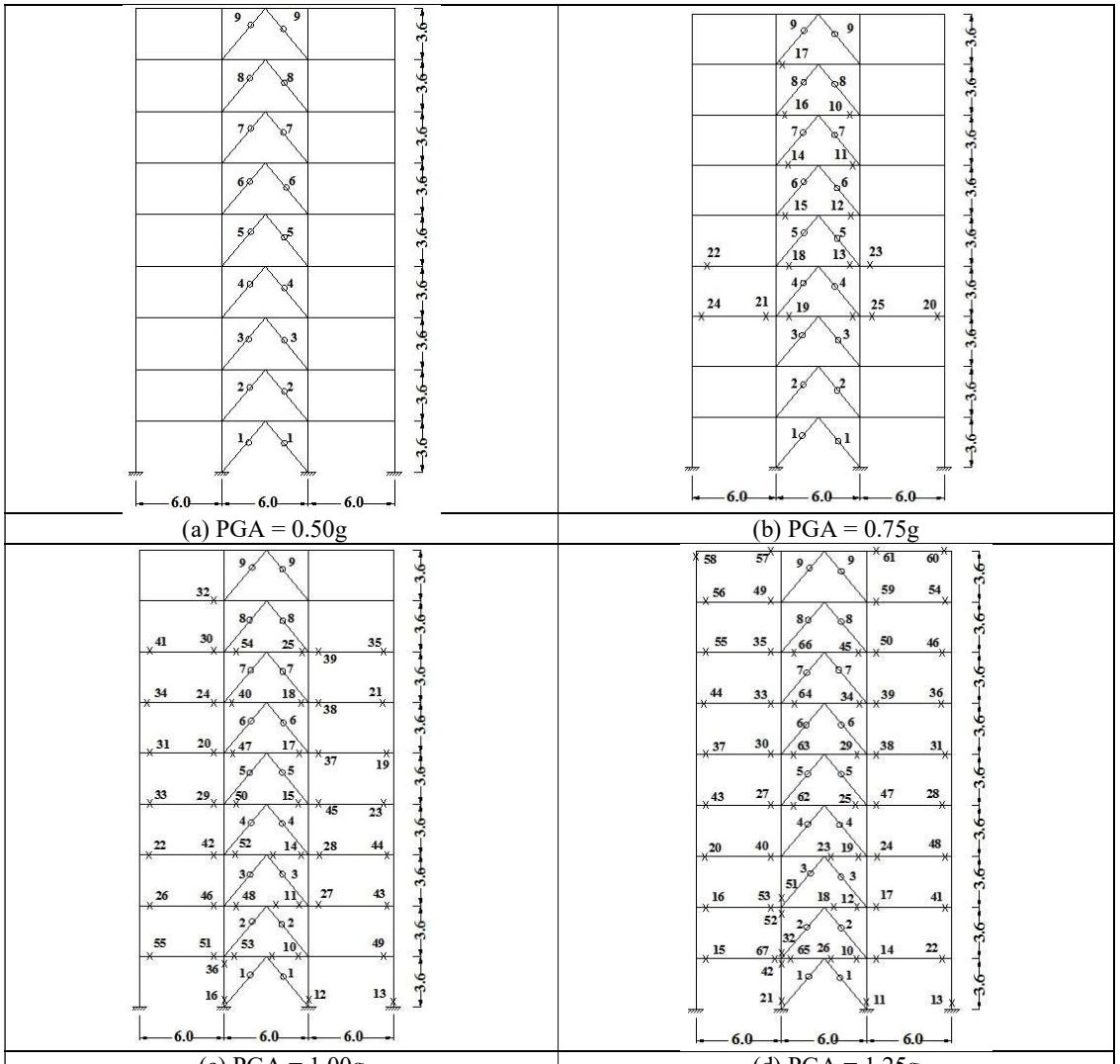

(a) PGA = 0.50g

(b) PGA = 0.75g

(c) PGA = 1.00g

(d) PGA = 1.25g

x : core concrete crushing o : yielding of bracing

Fig. 9: The sequence of core concrete crushing and yielding of bracing of Frame 3 (record no. 14)

4.3 Roof drift response

The variation of the "mean" and the "mean-plus-twice the standard deviation" of the Maximum Roof Drift Ratio (MRDR) of the three-and nine-story buildings with PGA are shown in Figs. 10a and 10b, respectively. The MRDR increases with the increase of PGA reaching values of 2.67% and 3.57% at PGA of 1.25g for Frames 1 and 3, respectively.

The mean values of the MRDR for Frames 2-6 and 4-18 at PGA of 1.25g were 2.97% and 3.89%, respectively. Using SMA reinforcing bars increased the MRDR by 11% and 9%, respectively. This may be attributed to the lower stiffness of the SMA bars in comparison with the steel bars. Similar increase was observed by Youssef and Elfeki (2012) for SMA RC frames.

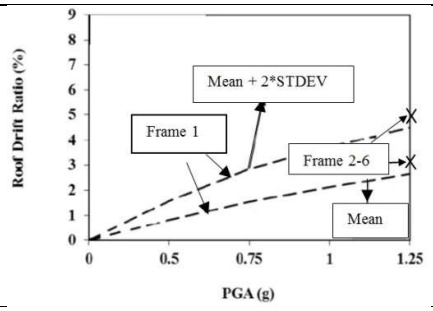

(a) Three-story building

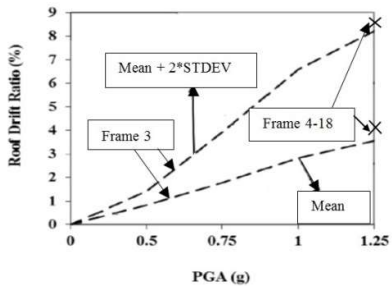

(b) Nine-story building

Fig. 10: Variation of the" mean" and the "mean-plus-twice the standard deviation" of the maximum roof drift ratio (MRDR) with PGA

4.4 Residual roof drift response

The variation of the "mean" and the "mean-plus-twice the standard deviation" of the Residual Roof Drift Ratio (RRDR) of the three-and nine-story buildings with PGA are shown in Figs. 11a and 11b, respectively. The RRDR increases with the increase of PGA reaching values of 0.12% and 0.31% at PGA of 1.25g for Frames 1 and 3, respectively.

The mean values of the RRDR for Frames 2-6 and 4-18 at PGA value of 1.25g were 0.06% and 0.15%, respectively. Using the SMA reinforcing bars reduced the RRDR by about 50% for both frames. This is mainly due to the re-centring capability of the SMA material.

4.5 Story drift response

The variation of the "mean" and the "mean-plus-twice the standard deviation" of the Maximum Story Drift Ratio (MSDR) of the three-and nine-story buildings with PGA are shown in Figs. 12a and 12b, respectively. The MSDR increases with the increase of PGA reaching values of 3.57% and 4.58% at PGA of 1.25g for Frames 1 and 3, respectively.

The mean values of the RRDR for Frames 2-6 and 4-18 at PGA of 1.25g were 3.82% and 5.05%, respectively. It is noted that using the SMA reinforcing bars increased the MSDR by about 11 % for both buildings and this may be attributed to the lower stiffness of the SMA bars as noted in roof drift section.

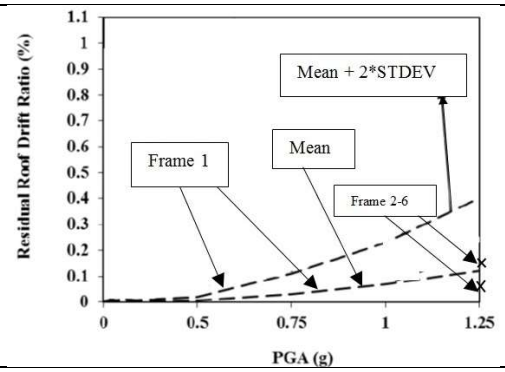

(a) Three-story building

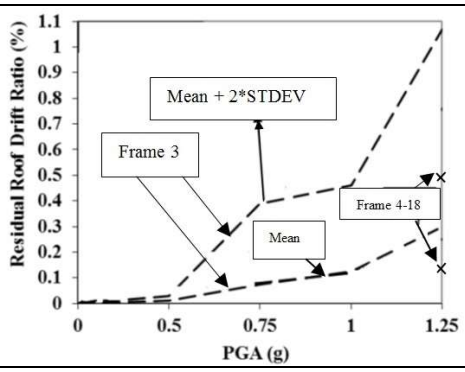

(b) Nine-story building

Fig. 11: Variation of the" mean" and the "mean-plus-twice the standard deviation" of the residual roof drift ratio (RRDR) with PGA

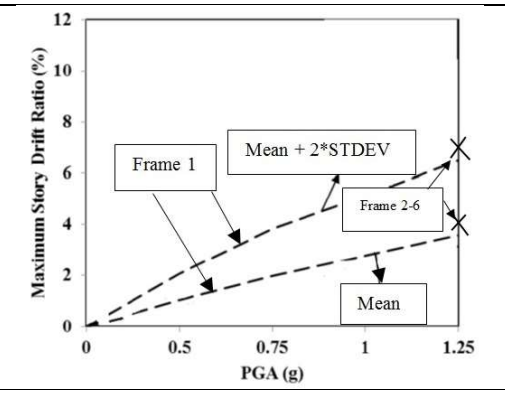

(a) Three-story building

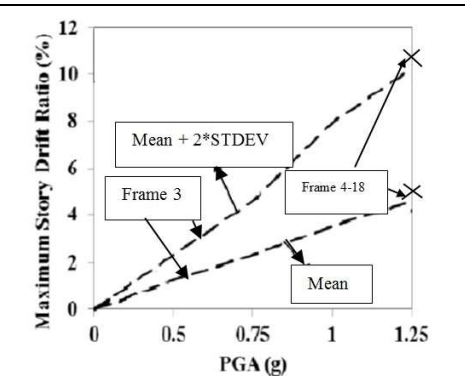

(b) Nine-story building

Fig. 12: Variation of the" mean" and the "mean-plus-twice the standard deviation" of the maximum story drift ratio (MSDR) with PGA

5. General observations

The seismic performance of Frames 1, 2-6, 3, and 4-18 at PGA of 1.25g are summarized in Table 6. The use of SMA bars has reduced the residual roof drifts by about 50%. However, it has increased the maximum drifts by about 10%. For SMA stacked chevron braces, locating SMA reinforcing bars at all of the expected plastic hinge locations seems to produce the highest reduction in seismic residual deformations. This conclusion differs from that by Youssef and Elfeki (2012) that address moment frames. The use of SMA bars in moment frames allowed redistribution of the moments, and thus was not required except at the frame critical locations. The performance of braced frames is controlled by the SMA braces and redistribution of moments did not impact their failure mechanism or PGA defining failure. The SMA bars reduced the residual

deformations at locations of their use and were deemed necessary at all of the plastic hinge locations.

Table 6: Seismic response of Frame 1, Frame 2-6, Frame 3, and Frame 4-18 at 1.25g

Frame	Maximum Roof Drift Ratio (MRDR) (%)		Residual Roof Drift Ratio (RRDR) (%)		Maximum Storey Drift Ratio (MSDR) (%)	
	Mean	Mean-plus-twice the standard deviation	Mean	Mean-plus-twice the standard deviation	Mean	Mean-plus-twice the standard deviation
1	2.67	4.77	0.12	0.40	3.57	6.50
2-6	2.97	4.97	0.06	0.16	3.82	7.07
3	3.57	8.21	0.31	1.07	4.58	10.26
4-18	3.89	8.65	0.15	0.52	5.05	11.23

6. Conclusion

This paper explored the effect of enhancing the seismic performance of SMA-braced Reinforced Concrete (RC) frames using SMA bars to reinforce the concrete beams. Three-story and nine-story SMA-braced Reinforced Concrete (RC) frames were designed utilizing regular steel reinforcing bars. Their seismic performance was examined using twenty seismic ground motions. The frames were then re-designed using SMA reinforcing bars. Different design alternatives representing different locations for the SMA reinforcing bars were considered. The use of SMA reinforcing bars did not affect the map of yielding and crushing for any of the buildings, however it reduced the residual roof drift ratio because of the re-centring capability of the SMA material. The residual roof drift ratio for both frames was reduced by about 50%. Using SMA bars at random locations might result in a slight increase in the residual deformations as observed in Frames 4-3 and 4-5.

Using SMA reinforcing bars increased the maximum roof drift ratio and the maximum story drift ratio. This increase was expected because of the lower stiffness of the SMA bars in comparison with steel bars. The maximum roof drift ratio and the maximum story drift ratio were increased by about 10%.

For reinforced concrete frames with SMA stacked chevron braces, the use of SMA reinforcing bars at all of the expected beam plastic hinge locations is expected to result in the lowest residual seismic deformations. These results are limited to the analysed cases and additional studies are needed to generalize them.

References

Alam M. S., Youssef M. A. and Nehdi M. (2008) “Analytical prediction of the seismic behaviour of superelastic shape memory alloy reinforced concrete elements”, *Engineering Structures*, **30**(12), 3399-3411.

Alam M. S., Nehdi M. and Youssef M. A. (2009) "Seismic performance of concrete frame structures reinforced with superelastic shape memory alloys", *Smart Structures and Systems*, **5**(5), 565-585.

Auricchio F. and Sacco E. (1997) "A superelastic shape-memory-alloy beam", *Journal of Intelligent Materials and Structures*, **8**(6), 489-501.

Auricchio F., Fugazza D., DesRoches, R. (2006) "Earthquake performance of steel frames with nitinol braces", *Journal of Earthquake Engineering*, 1**0**(1), 45-66.

Asgarian B. and Moradi S. (2011) "Seismic response of steel braced frames with shape memory alloy braces", *Journal of Constructional Steel Research*, **67**(1), 65-74.

Mander J.B., Priestley M.J.N. and Park R. (1988) "Theoretical stress-strain model for confined concrete", *Journal of Structural Engineering*, **114**(8), 1804-1826.

Martinez-Rueda J.E. and Elnashai A.S. (1997) "Confined concrete model under cyclic load", *Materials and Structures*, **30**(197), 139-147.

McCormick J., and DesRoches R. (2003) "Seismic response reduction using smart bracing elements", Extreme Loadings Conference: Response of Structures to Extreme Loadings, Toronto.

Saiidi M.S., and Wang H. (2006) "Exploratory study of seismic response of concrete columns with shape memory alloys reinforcement", *ACI Structural Journal*, **103**(3), 435-442.

Saiidi, M.S., O'Brien, M., Mahmoud, S.Z. (2009) "Cyclic response of concrete bridge columns using superelastic nitinol and bendable concrete", *ACI Structural Journal*, **106**(1), 69-77

Saiidi, M., Sadrossadat-Zadeh, M., Ayoub, C., and Itani, A. (2007). "Pilot Study of behavior of Concrete Beams Reinforced with Shape Memory Alloys", *Journal of Materials in Civil Engineering*, **19**(6), 454–461.

Vamvatsikos, D. and Cornell, C. A. (2004) "Applied incremental dynamic analysis", *Earthquake Spectra*, **20**(2), 523-555.

Youssef M. A. and Elfeki M.A. (2012) "Seismic performance of concrete frames reinforced with superelastic shape memory alloys", *Smart Structures and Systems*, **9**(4), 313-333.

Youssef M.A., Alam M.S., Nehdi M. (2008) "Experimental investigation on the seismic behavior of beam-column joints reinforced with superelastic shape memory alloys", *Journal of Structural Engineering*, **12**(7), 1205 – 1222.

Paulay T. and Priestley M.J.N. (1992), *Seismic Design of Reinforced Concrete and Masonry Buildings*, John Wiley & Sons, New York.

ACI Committee 318, (2008). *Building code requirements for structural concrete*, (ACI 318-08) and commentary (ACI 318R-08), American Concrete Institute, Farmington Hills, MI.

IBC (2009). *International building code*, International code council, Country Club Hills, IL.

SeismoStruct (2009), Version 4.0.2. accessed on Feb 2009, available at http://www.seismosoft.com/SeismoStruct/index.htm.

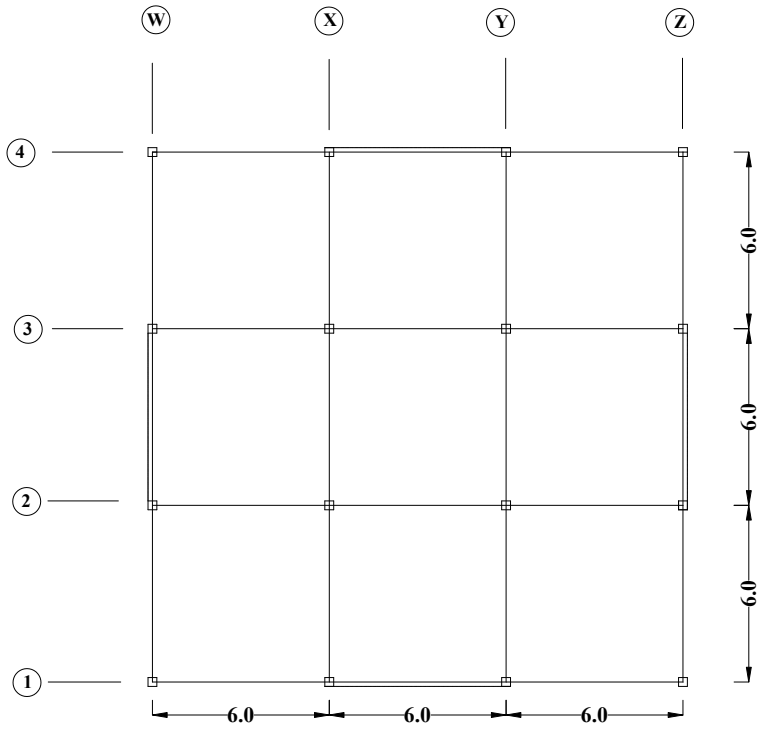

(a) Plan view

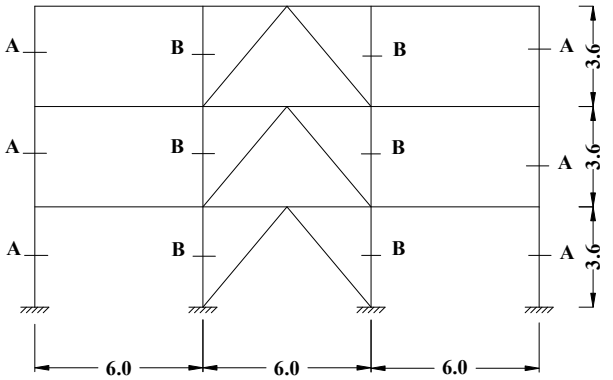

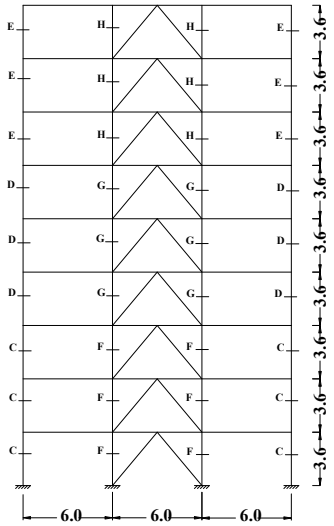

(b) Elevation of the three-story building (c) Elevation of the nine-story building

Fig. 1 RC braced frames (All dimensions are in meters)

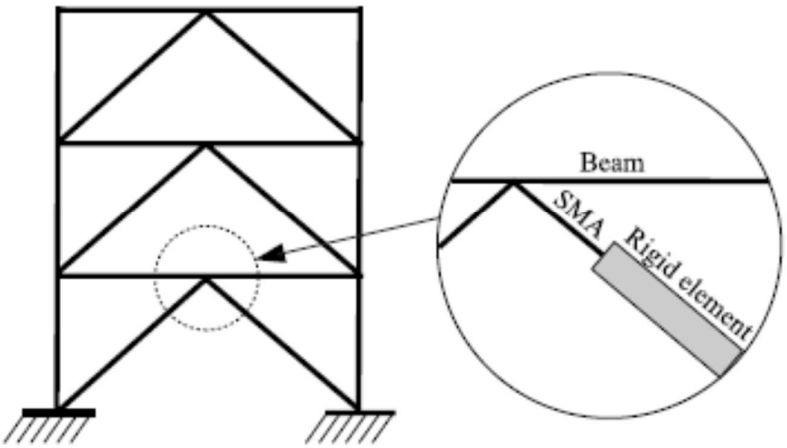

Fig. 2 Components of SMA Brace

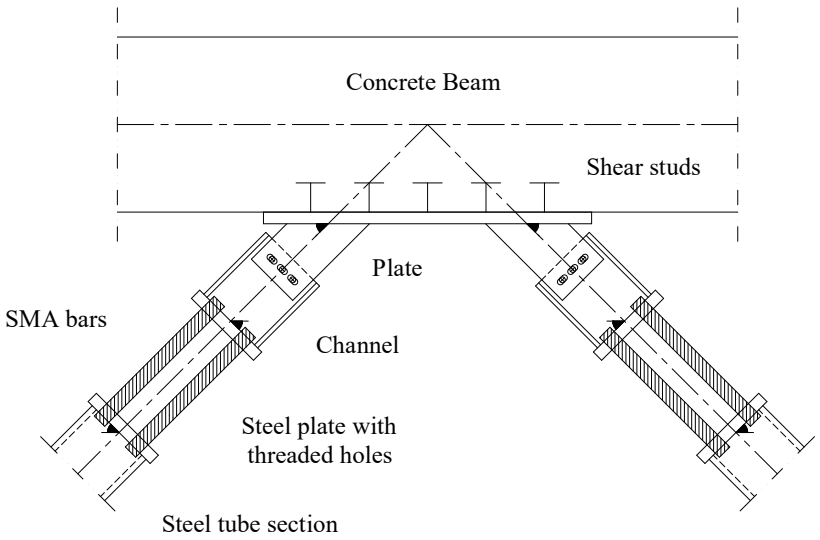

Fig. 3 Potential Connection Detail for SMA Braces

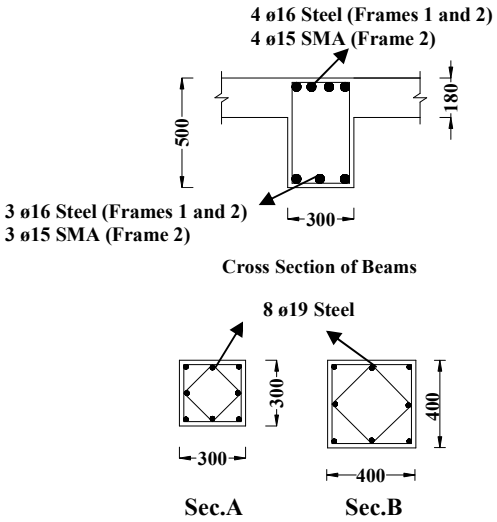

(a) Details of Frames 1 and 2

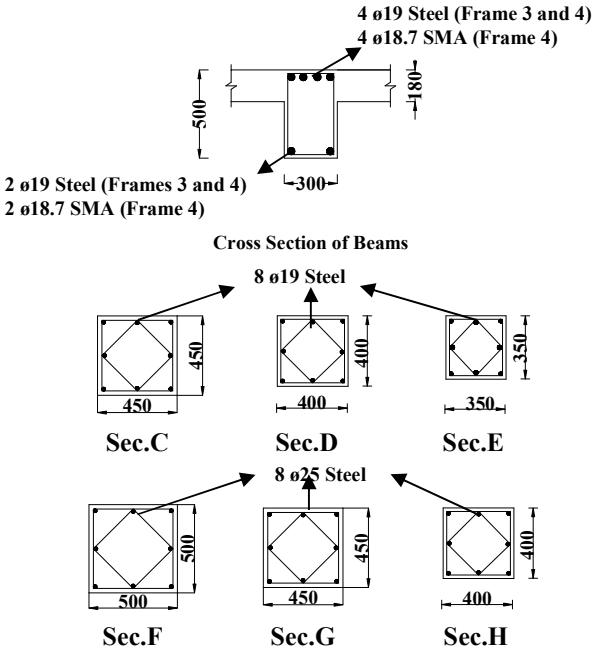

(b) Details of Frames 3 and 4

Fig. 4 Sections of the designed frames

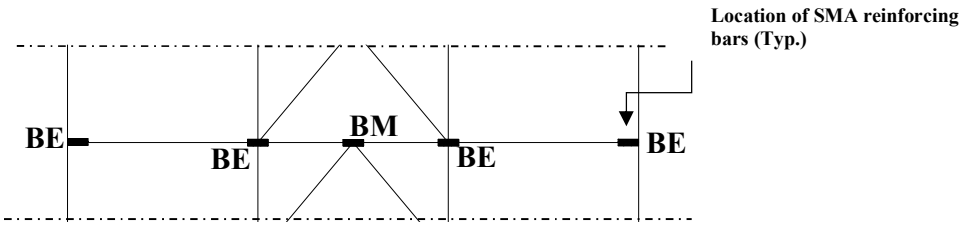

Fig. 5 Schematic Diagram for potential locations of SMA reinforcing bars

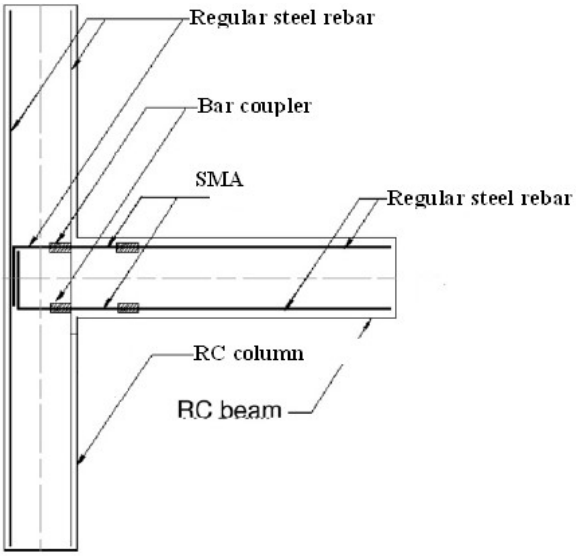

Fig. 6: Detail of a beam column joint

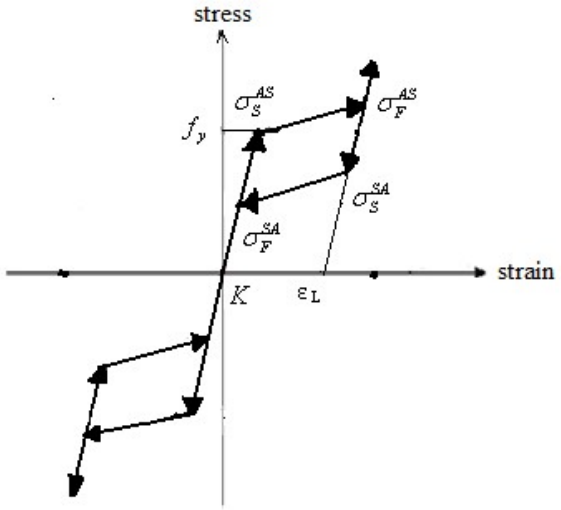

Fig. 7: The superelastic SMA model (Auricchio et al. 2006)

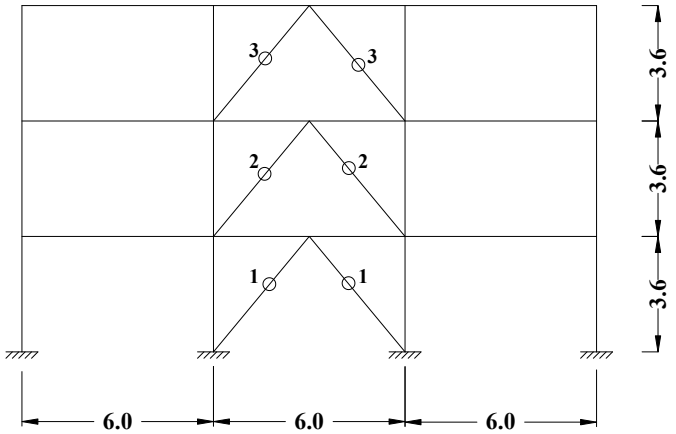

(a) PGA = 0.50g

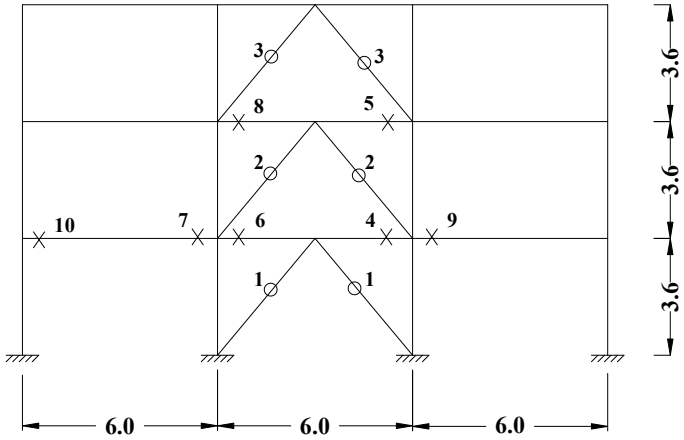

(b) PGA = 0.75g

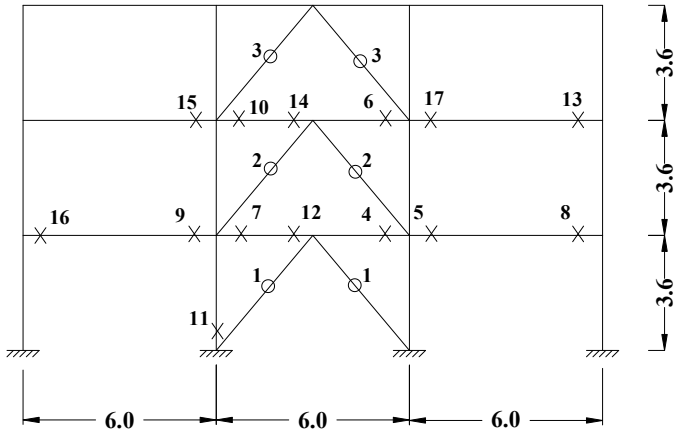

(c) PGA = 1.00g

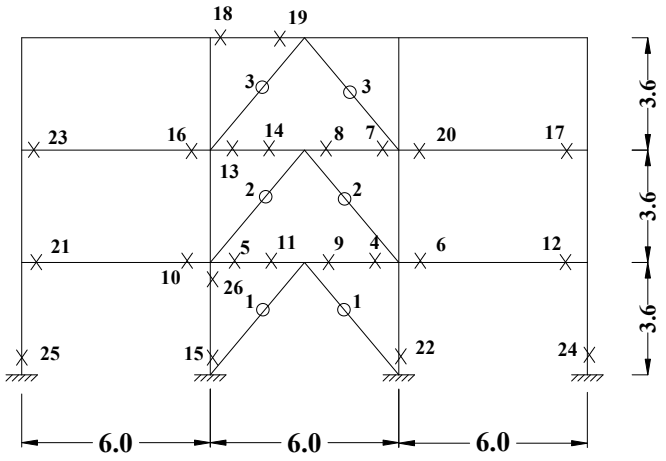

(d) PGA = 1.25g

x : core concrete crushing o : yielding of bracing

Fig. 8: The sequence of core concrete crushing and yielding of bracing of Frame 1 (record no. 18)

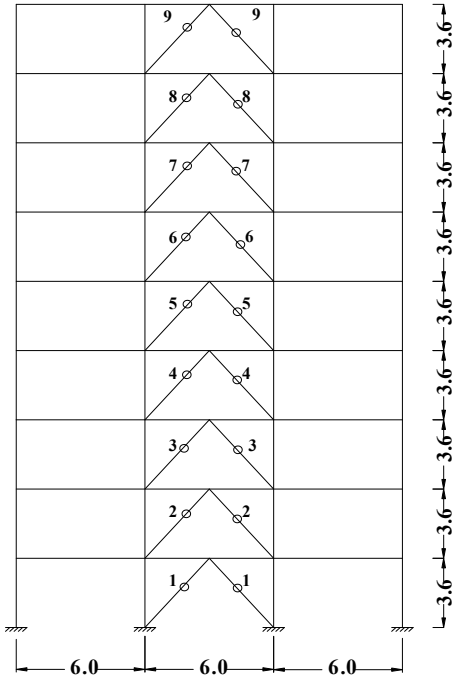

(a) PGA = 0.50g

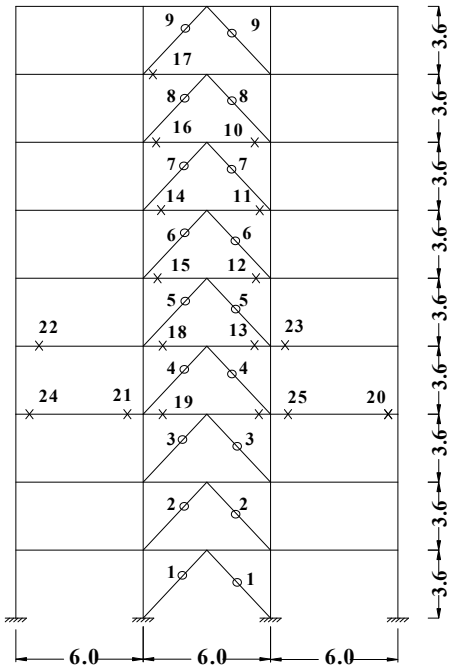

(b) PGA = 0.75g

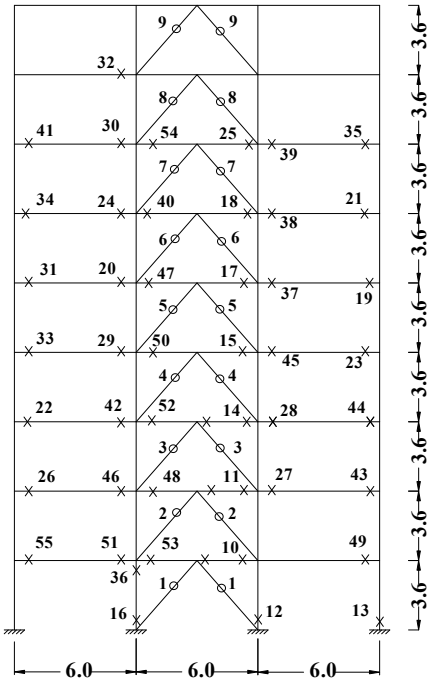

(c) PGA = 1.00g

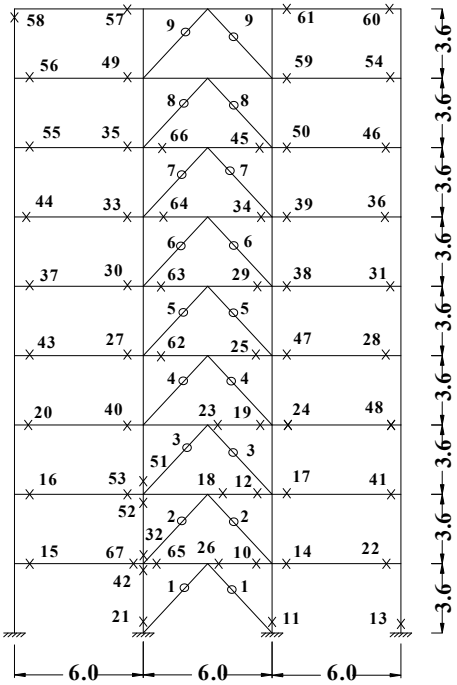

(d) PGA = 1.25g

x : core concrete crushing o : yielding of bracing

Fig. 9: The sequence of core concrete crushing and yielding of bracing of Frame 3 (record no. 14)

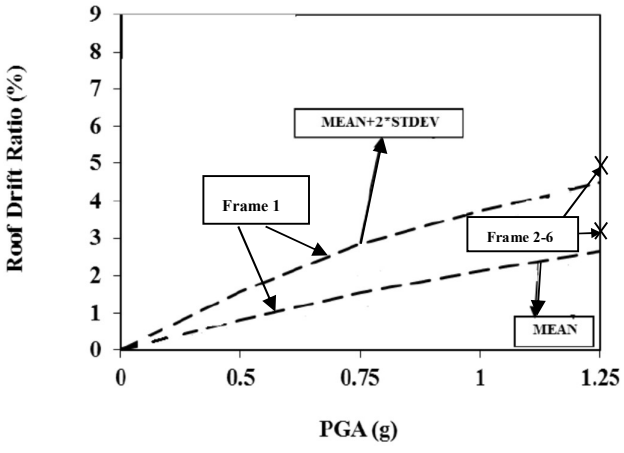

(a) Three-story building

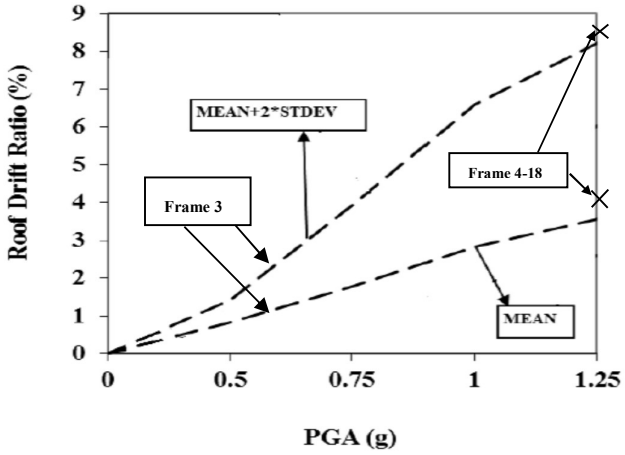

(b) Nine-story building

Fig. 10: Variation of the" mean" and the "mean-plus-twice the standard deviation" of the maximum roof drift ratio (MRDR) with PGA

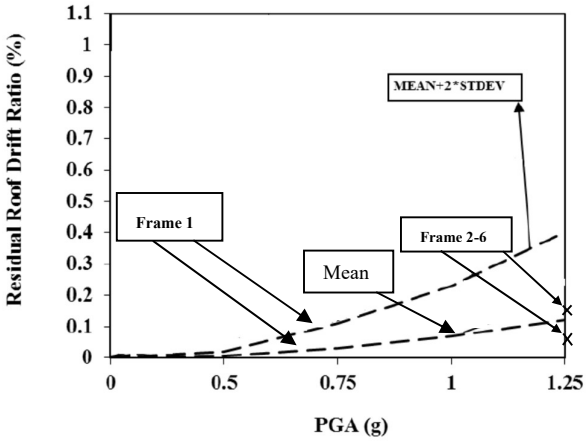

(a) Three-story building

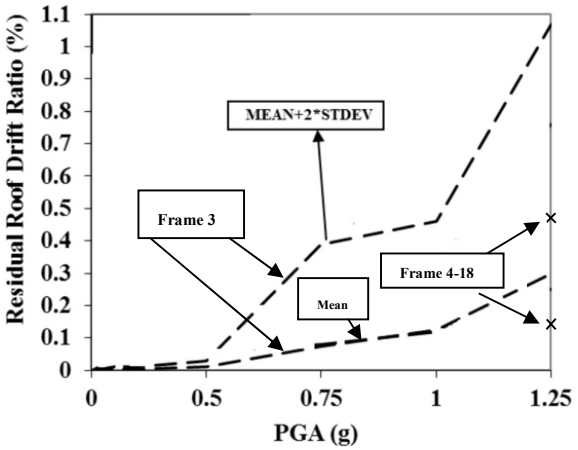

(b) Nine-story building

Fig. 11: Variation of the" mean" and the "mean-plus-twice the standard deviation" of the residual roof drift ratio (RRDR) with PGA

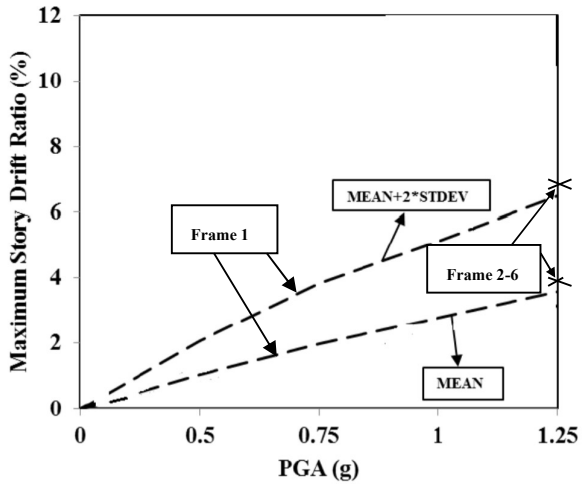

(a) Three-story building

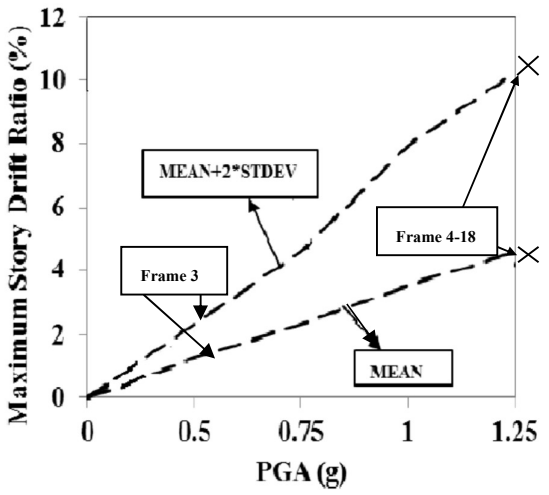

(b) Nine-story building

Fig. 12: Variation of the" mean" and the "mean-plus-twice the standard deviation" of the maximum story drift ratio (MSDR) with PGA